Clays and Clay Minerals, Vol. 50, No. 4, 455–469, 2002.

INFRARED STUDY OF REDUCED AND REDUCED-REOXIDIZED FERRUGINOUS SMECTITE

CLAIRE-ISABELLE FIALIPS, DONGFANG HUO, LAIBIN YAN, JUN WU AND JOSEPH W. STUCKI*

Department of Natural Resources and Environmental Sciences, University of Illinois, 1102 South Goodwin Avenue, Urbana, Illinois 61801

Abstract—Oxidation-reduction processes within natural systems greatly influence the properties of sediments, soils and clays. The objective of this experimental study was to gather new evidence for the effects of changes in redox conditions (reduction and reoxidation) on structural properties of ferruginous smectite and to understand better the mechanisms involved. The <2 μm fraction of a ferruginous smectite (sample SWa-1), which contains 17.3 wt.% of total structural Fe, was studied by infrared (IR) spectroscopy. The pure Na-saturated clay was reduced by Na dithionite for 10 to 240 min to obtain various Fe(II):(total Fe) ratios ranging from 0 to 1.0. Selected reduced samples were then reoxidized completely by bubbling O_2 gas through the suspensions for up to 12 h. Infrared spectra of the initially unaltered, reduced and reduced-reoxidized samples were collected. Reduction generated changes in the three studied spectral regions (O−H stretching, *M*−O−H deformation, and Si−O stretching), indicating that major modifications occurred within the clay crystal beyond merely a change in Fe oxidation state. Partial dehydroxylation and redistribution of Fe, and perhaps Al, cations occurred upon reduction of SWa-1, changing the structural properties of its tetrahedral and octahedral sheets. Water molecules, probably generated by dehydroxylation within the octahedral sheet upon reduction, were tightly bound to the clay surface and were possibly trapped within the clay structure. Except for dehydroxylation and the Fe oxidation state, all these modifications were largely irreversible. The tightly bound water was not completely removed upon reoxidation and the cationic rearrangements generated during reduction were not reversed: either they were preserved as in the reduced state or cations were redistributed into a different configuration from the unreduced clay.

Key Words—Cationic Rearrangement, Infrared Spectroscopy, Iron, Irreversibility, OH Stretching, OH Deformation, Reduction, Reoxidation, Si−O Stretching, SWa-1 Smectite.

INTRODUCTION

Chemical reduction of structural Fe in ferruginous smectite and nontronite has been studied widely for more than three decades (*e.g.* Roth *et al.*, 1969; Stucki and Roth, 1976, 1977; Rozenson and Heller-Kallai, 1976a, 1976b; Stucki *et al.*, 1984a, 1984b, 1984c, 1996, 2000; Russell *et al.*, 1979; Lear and Stucki, 1985, 1989; Chen *et al.*, 1987; Wu *et al.*, 1989; Komadel *et al.*, 1990, 1995; Khaled and Stucki, 1991; Shen *et al.*, 1992; Yan and Stucki, 1999, 2000; Manceau *et al.*, 2000b; Drits and Manceau, 2000). Results indicate that structural Fe(III) reduction generates partial dehydroxylation and other changes in clay properties (magnetic ordering, layer stacking, crystallinity, texture, surface charge, *etc.*). Stucki and Roth (1977) observed that the increase of surface charge is non-linearly related to the amount of Fe reduced, and proposed that some of the increased negative charge was compensated by the loss of structural OH groups. Hence, prediction of property changes must rely on more than the observed change in Fe oxidation state. Presumably, the crystal structure changes in order to accommodate the larger size of Fe(II) and the increased negative charge. To understand changes in physical and chemical properties of clays when subjected to redox conditions, we must first understand changes occurring within their structure.

Numerous studies of the effect of Fe oxidation state on the crystal structure of Fe-bearing clays were limited to ~50% of total Fe actually reduced, and reduced samples were often unprotected from reoxidation (Roth *et al.*, 1969; Roth and Tullock, 1973; Rozenson and Heller-Kallai, 1976a, 1976b; Russell *et al.*, 1979). Since the 1980s, Stucki and co-workers have focused on higher levels of Fe reduction, achieved through careful use of inert-atmosphere techniques and by removing gaseous reaction products during Fe reduction (*e.g.* Stucki *et al.*, 1984a; Komadel *et al.*, 1990). In spite of past studies and growing interest in this subject (Ernsten *et al.*, 1998; Hunter *et al.*, 1999; Yan and Stucki, 1999, 2000; Drits and Manceau, 2000; Manceau *et al.*, 2000a, 2000b; Stucki *et al.*, 2000; Favre *et al.*, 2002; Fialips *et al.*, 2002; Nzengung *et al.*, 2001), we still have much to learn about the relationships existing between the nature of the clay, its Fe(II):Fe(III) ratio, its crystal structure, and its chemical and physical properties. Several experimental studies (Stucki and Roth, 1977; Stucki *et al.*, 1984b; Lear and Stucki, 1985) showed that reduction of structural Fe(III) in dioctahedral smectites increases significantly their surface charge and cation exchange capacity (CEC). To cast this result into the form of a

* E-mail address of corresponding author:
jstucki@uiuc.edu

reaction mechanism, Stucki and Roth (1977) proposed the following sequence:

$$m\ \mathrm{Fe(III)_x} + m\ (\mathrm{e^-})_s \rightarrow m\ \mathrm{Fe(II)_x};\ 2n\ [\mathrm{OH^-}]_x \rightarrow n\ [\mathrm{O^{2-}}]_x + n\ \mathrm{H_2O_s};\ n\ [\mathrm{O^{2-}}]_x + n\ [\mathrm{H^+}]_s \rightarrow n\ [\mathrm{OH^-}]_x \quad (1)$$

where x and s denote the solid and solution phases, respectively, and m and n are stoichiometric parameters. Water molecules would be formed from dehydroxylation and the residual oxygen atoms would form OH groups by protonation from solution. The layer charge of the smectite in this model depends on the number of OH groups that undergo dehydroxylation (*i.e.* n). Lear and Stucki (1985) determined that n/m equals 0.32. But because these models predict a greater increase in layer charge than is actually observed, Stucki and Lear (1989) introduced the idea that electron-rich centers within the smectite (such as Al-substituted tetrahedral sites) could be a source for further structural Fe reduction, resulting in the formation of Fe(II) without a change in layer charge.

Though these models are generally in agreement with the loss of OH groups observed experimentally upon reduction and with the variation in layer charge, they imply a transformation of ^{VI}Fe coordination from six-fold to five-fold. Manceau *et al.* (2000b) demonstrated by X-ray powder diffraction (XRD) and polarized extended X-ray absorption fine-structure (P-EXAFS) spectroscopy that ^{VI}Fe in reduced smectites is purely six-fold coordinated. Drits and Manceau (2000) summarized and discussed the different models proposed since the 1970s for the reduction of Fe-bearing smectites using sodium dithionite, and proposed a new model which attempted to take into account the dehydroxylation, the increase in layer charge, and the fact that ^{VI}Fe keeps its six-fold coordination. They proposed the following sequence:

$$m\ \mathrm{Fe(III)_x} + m\ (\mathrm{e^-})_s \rightarrow m\ \mathrm{Fe(II)_x};\ w_0\ \mathrm{Na_x} + p\ \mathrm{Na_s} \rightarrow w\ \mathrm{Na_x};\ n\ [\mathrm{OH^-}]_x + n\ [\mathrm{H^+}]_s \rightarrow n\ \mathrm{H_2O_s} \quad (2)$$

where x and s denote the solid and solution phases, respectively; w and w_0 correspond to interlayer Na content in the reduced and unreduced states, respectively; m and n are stoichiometric parameters, $m = p + n$; and $w = w_0 + p$. This reaction model is in agreement with the structural model proposed by Manceau *et al.* (2000b) for reduced nontronite, implying that Fe retains its six-fold coordination and each pair of edge-forming OH groups coordinated to ^{VI}Fe(II) forms 2 H_2O molecules by protonation while the ^{VI}Fe(II) migrates from *cis*- to *trans*-octahedral sites along the [010] direction. However, it implies that previous studies failed to measure total and exchangeable Na correctly and, thus, reported erroneous changes in silicate layer charge. New experimental data for the extent of dehydroxylation and other changes occurring within the clay structure upon reduction, and the reversibility of these changes upon reoxidation, are required to further clarify these models.

The aim of the present work was to characterize changes in IR spectra of a ferruginous smectite (SWa-1) after different levels of Fe(III) reduction and subsequent reoxidation. The IR regions of O−H stretching, *M*−O−H deformation, and Si−O stretching were studied to understand changes occurring upon reduction within the clay structure and to determine the extent of reversibility of these modifications upon reoxidation. Results will contribute to a better knowledge of reduction-reoxidation processes, and of the relations existing between the clay properties and the redox conditions.

MATERIALS AND METHODS

Clay preparation

The clay studied was the <2 μm fraction of ferruginous smectite (sample SWa-1 from Grant County, Washington, obtained from the Source Clays Repository of The Clay Minerals Society, Columbia, Missouri). The clay was purified using the same method as Huo (1997) and Fialips *et al.* (2002) which, unlike conventional clay fractionation by sedimentation or centrifugation (Jackson, 1979), is effective for the removal of fine-grained silica and Fe oxides. Briefly, this method consisted of successive dispersions in 1 M NaCl solution or pure water, separated by short centrifugations at progressively increased speeds (10,000 rpm up to 15,000 rpm; Dupont Model Sorvall RC 5C plus centrifuge with SS-34 rotor) and removal of any impurity settled to the bottom of the centrifuge tubes, resulting in a salt-free and Na-saturated sample which was then freeze dried for storage. It was yellowish green in color and its XRD pattern was typical of pure Fe-rich smectite (data not shown). The unit-cell formula proposed by Manceau *et al.* (2000a) for the pure Na-saturated SWa-1 is:

$$\mathrm{Na_{0.87}(Si_{7.38}Al_{0.62})(Fe^{3+}_{2.67}Fe^{2+}_{0.01}Al_{1.08}Mg_{0.23})O_{20}(OH)_4}.$$

Reduction and reoxidation of structural Fe

A buffer solution was prepared by mixing two parts of 1.2 M sodium citrate ($Na_3C_6H_5O_7{\cdot}2H_2O$) and 1 part of 1 M sodium bicarbonate ($NaHCO_3$). A measured amount of SWa-1 (30−50 mg) was dispersed in 20 mL of deionized water in an inert-atmosphere reaction vessel (Stucki *et al.*, 1984a), then 10 mL of the buffer solution were quickly added and the temperature was held at 70°C using a water bath. Structural Fe was reduced by adding sodium dithionite ($Na_2S_2O_4$) in the ratio of 100 mg of $Na_2S_2O_4$ to 30 mg of clay, and four different Fe(II):(total Fe) atomic ratios (0.2 to ~1.0) were obtained by selecting reduction periods of 10, 30, 60 or 240 min. The reduced samples were washed once with and redispersed in deionized O_2-free water. Reduced-reoxidized samples were obtained by bubbling O_2 gas through the suspensions, at 70°C, for 8 to 12 h. These

conditions were chosen because they proved to be efficient to maximize the conversion back to Fe(III) for other reduced Fe-rich smectites (Huo, 1997; Yan and Stucki, 1999; Fialips *et al.*, 2002).

Photochemical analyses

The actual Fe(II):(total Fe) atomic ratios of the reduced and reduced-reoxidized smectites were measured by visible spectrophotometry (Beckman UV-visible spectrophotometer, Model 5230, 510 nm wavelength) using the 1,10-phenanthroline (phen) method (Stucki, 1981; modified by Komadel and Stucki, 1988). The Fe(II) concentration was first determined by measuring under red light the $Fe(phen)_3^{2+}$ complex formed during HF-H_2SO_4 digestion of the mineral in the presence of 1,10-phenanthroline. Then, the total Fe was measured after conversion of any μ-oxo-$Fe_2(phen)_4^{6+}$ in the digestate to $Fe(phen)_3^{2+}$ by photochemical reduction using a mercury vapor lamp.

Infrared spectroscopy

Data acquisition. The unaltered (unreduced), reduced and reduced-reoxidized SWa-1 samples were analysed by IR spectroscopy, using a Midac M-2000 FTIR spectrometer, combined with the Grams/386 program for data acquisition and processing. The spectrometer was purged constantly with dry N_2 gas. The IR spectra were recorded in transmission mode, from 400 to 4000 cm^{-1}, with a nominal resolution of 1 cm^{-1}. In the spectral ranges of structural O–H stretching and deformation (*i.e.* 3000–3800 and 550–950 cm^{-1}, respectively), IR spectra were collected from self-supporting films, mounted on holders with a 15 mm diameter hole. The actual mass of each film was measured and the peak intensity of each spectrum was normalized to a sample mass of 10 mg/film. In the spectral range of Si–O stretching (*i.e.* 800–1300 cm^{-1}), IR spectra were collected from clay deposits on ZnSe windows. No weight normalization was possible in this IR range. For an easy comparison of the positions of the Si–O bands, the maximum absorption intensity of each spectrum was normalized to an arbitrarily chosen value.

Preparation and handling of clay films and window deposits. Diluted clay suspensions (~75 mL, containing 4 to 13 mg of smectite sample) were filtrated at low pressure (20 psi during 2 h and 30 psi during 40 min) using a mini-pressure plate apparatus with a Millipore membrane filter (Stucki *et al.*, 1984c). The wet self-supporting films were peeled from the filter membranes and dried. To prepare window deposits, 1 mL of clay suspension (containing ~2 mg of clay) was deposited onto a ZnSe polished disc (25 mm in diameter and 2 mm in thickness) and dried. The films and window deposits of the unreduced and reoxidized samples were prepared under ambient conditions and kept in a desiccator containing P_2O_5 for ~24 h to remove the adsorbed H_2O before data acquisition. The films and window deposits of the reduced samples were prepared inside a glove box under an Ar atmosphere (<1 ppm O_2) to prevent reoxidation. They were evacuated in the ante-chamber of the glove box for a few hours to remove excess adsorbed H_2O. Finally, they were transferred to a sealed vacuum cell prior to removal from the glove box for IR spectral acquisition to prevent reoxidation and rehydration. Most of the IR spectra were collected without removing the clay preparations from the sealed vacuum cell, but the window material of the vacuum cell (ZnSe) is opaque to IR radiation at energies <650 cm^{-1}. Thus, during spectral acquisitions in this range, the self-supporting films were placed directly into the sample chamber, with the dry N_2 purge being the only protection from the atmosphere. These spectra were collected rapidly (<5 min) and the Fe(II):(total Fe) ratio was checked after data collection. This brief exposure of dried films to the atmosphere resulted in no measurable change in oxidation state.

Deconvolution of the IR spectra. Deconvolution of the IR spectra of the unaltered, reduced and reduced-reoxidized samples in the OH-stretching and deformation regions was realized using the Grams/32 computing software (version 4.11, Galactic Industries Corporation, Salem, NH). The IR spectra were fitted using mixed Gaussian-Lorentzian bands. The Gaussian-Lorentzian mixing ratios, position, width, and intensity of each component band were generally left variable, but were sometimes restrained within a specific range to obtain a satisfactory fitting (coherent component shape and position, small minimization function χ^2, function R^2 close to 1.000, and good agreement between experimental and calculated profiles).

RESULTS AND DISCUSSION

Fe(II):(total Fe) ratio and color changes

Drastic changes in color of the clay suspensions were observed upon reduction. As the time of reduction increased (*i.e.* as the Fe(II) content increased) up to 240 min, the color changed progressively from the yellowish green color to emerald green, blue-green, dark blue, light blue, gray and light gray. The exact same sequence of color changes was observed previously by Komadel *et al.* (1990) upon reduction of three other nontronites. Changes in color during reduction often provide a good estimate of the reduction levels (Anderson and Stucki, 1979; Lear and Stucki, 1987; Komadel *et al.*, 1990; Huo, 1997), the gray color indicating a complete or almost complete reduction of Fe(III) to Fe(II) (*e.g.* Komadel *et al.*, 1990; Huo, 1997). For the 240 min reduced SWa-1, a small amount of dissolved Fe was found in the supernatant solution.

The Fe(II):(total Fe) ratio of the unreduced, reduced and reduced-reoxidized samples are given in Table 1.

The Fe(II):(total Fe) ratio of reduced SWa-1 samples increased significantly but was non-linear with reduction time, as already observed by Anderson and Stucki (1979), Lear and Stucki (1987), Komadel *et al.* (1990) and Fialips *et al.* (2002) for reduced nontronites. Although using the same method of reduction, the reduction of the SWa-1 smectite is significantly faster than that of the Garfield nontronite. After 10 min of reduction, the Fe(II):(total Fe) ratio already reached 0.33 for SWa-1, while it was only 0.2 for Garfield (Fialips *et al.*, 2002). One explanation for this observation may be that, unlike Garfield, SWa-1 consists primarily of very small particles (mostly <0.5 μm). One could argue that the difference in Fe reduction between SWa-1 and Garfield could be due to the presence of goethite in SWa-1 (Manceau *et al.*, 2000a), but the purification method we used was sufficient to remove goethite from our sample: no trace of goethite was observed by XRD and Mössbauer (data not shown). Hereafter, reduction levels will be identified by reduction period (*i.e.* 0, 10, 30, 60 or 240 min) instead of by the Fe(II):(total Fe) ratio.

After reoxidation, almost all Fe(II) was converted back to Fe(III) (Table 1, Fe(II):(total Fe) $\leqslant 0.01$), but the color of the reoxidized sample differed from that of the original (unaltered) clay by varying degrees. The shorter the time of reduction, the closer the reoxidized color was to the original, ranging from yellowish green for the 10 min reduced sample to brown for the 240 min reduced sample. The obvious color difference between unaltered and reoxidized samples suggested a disruption in the crystal structure during reduction, and indicated the irreversibility of the process. The brown color after reoxidation of the 240 min reduced samples may indicate that a poorly-crystalline Fe oxide phase was formed during or after reoxidation. This would require the release of some Fe from the clay crystal structure during the reduction-reoxidation process. As indicated earlier, we noticed the presence of a small amount of Fe in the supernatant solution after 240 min of reduction, but the buffer used during the reduction (sodium citrate) was concentrated enough to complex all dissolved Fe. No Fe oxide precipitation was then possible during the reduction process (Stucki *et al.*, 1984b). Each reduced sample was washed before reoxidation. If any Fe oxide was present in the 240 min reduced-reoxidized sample, this admixed phase had to be formed during the reoxidation process only.

IR spectra in the 600–950 cm^{-1} region

Infrared analysis of unaltered SWa-1 (0 min reduction, Figure 1) clearly revealed two intense $M-O-H$ deformation bands (where M = Al or Fe) at ~876 and ~824 cm^{-1} which are assigned to AlFe(III)OH and $[Fe(III)]_2OH$ deformations, respectively (Serratosa, 1960; Stubican and Roy, 1961; Farmer and Russell, 1964; Russell *et al.*, 1970; Farmer, 1974). These two bands reflect the high proportions of Fe(III) and Al in octahedral sites, as indicated also by the structural formula which gives 2.67 atoms of Fe(III) and 1.08 of Al per formula unit (a.p.f.u.). The results of one possible decomposition of the spectrum of unaltered SWa-1 (0 min reduction) in the *M*OH-deformation range are presented in Table 2 and Figure 2. The 875 cm^{-1} band appears much more intense than the 822 cm^{-1} band, suggesting that Fe-Al pairs rather than Fe-Fe pairs dominate the Fe environment in the octahedral sheet. However, the relative intensities of the AlFe(III)OH and $[Fe(III)]_2OH$ vibration bands observed by Gates *et al.* (2002) in the near infrared (NIR) spectrum of SWa-1 between 4300 and 4500 cm^{-1} indicate the opposite. The shape of the baseline and the overlapping bands due to these characteristic deformation modes in the 750 to 950 cm^{-1} mid-infrared (MIR) range hinder the accurate decomposition of the spectrum and could account for some of this discrepancy. The absorptivity of the different $M-O-H$ deformation bands could, however, be different: the intensity of the AlFeOH and Fe_2OH bands would then inaccurately reflect the actual concentration of these two groupings.

Three shoulders are also observed in the *M*OH-bending region of the unaltered SWa-1: at ~921, ~849 and ~792 cm^{-1} (Figure 1). The 921 cm^{-1} shoulder is generated by a band located at 919 cm^{-1} (Table 2, Figure 2) assigned to Al_2OH deformations (Farmer and Russell, 1964). Its low intensity relative to the 876 cm^{-1} band suggests that Fe-Al pairs rather than Al-Al pairs dominate the Al environment in the octahedral sheet. The 792 cm^{-1} shoulder is due to a band located at 788 cm^{-1} (Table 2, Figure 2) which was attributed to Fe(III)MgOH deformation by Farmer (1974) and Goodman *et al.* (1976). However, a more intense 790 cm^{-1} band is present in the spectrum of Garfield nontronite (Fialips *et al.*, 2002) despite the fact that it contains a negligible amount of Mg. Another possible assignment of this band is to a small amount of amorphous silica, which, in spite of the extended

Table 1. Measured Fe(II) content in unaltered (unreduced), reduced and reduced-reoxidized ferruginous smectite (SWa-1), expressed as a percentage of total Fe.

Reduction time	0 min	10 min	30 min	60 min	240 min
Reduced SWa-1	0.3	32.9	67.0	82.3	97.1
Reoxidized SWa-1	–	0.7	0.9	0.9	1.0

Note: errors associated with each value are $\leqslant 5\%$ of the value.

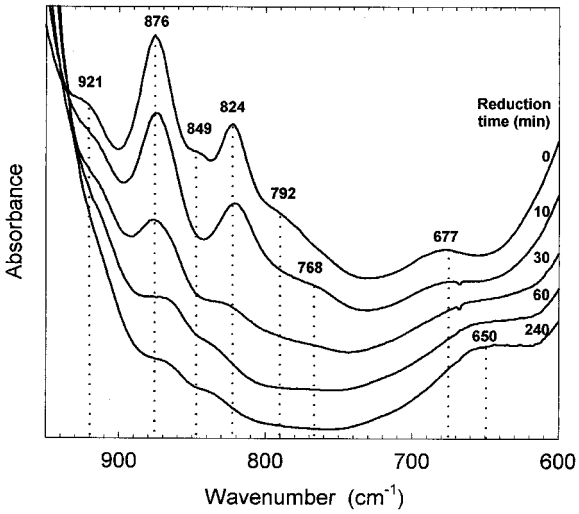

Figure 1. Normalized IR spectra in the OH-deformation region of the SWa-1 nontronite initially unreduced, and reduced for periods varying from 10 to 240 min with sodium dithionite.

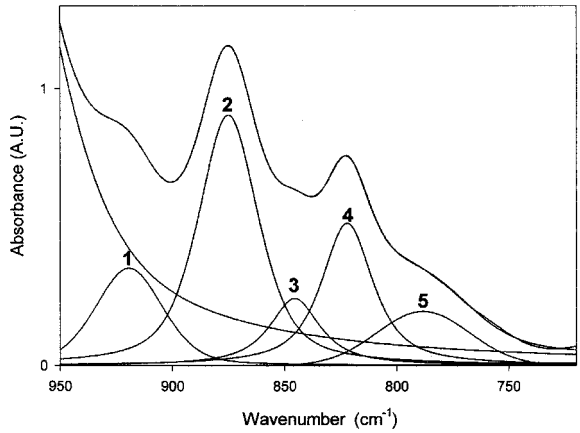

Figure 2. Deconvolution of the unaltered SWa-1 IR spectrum into several components (see Table 2) in the OH-deformation range; experimental and calculated curves.

purification process for SWa-1, could still be present; but, as discussed below, this assignment is unlikely.

Several authors (*e.g.* Petit *et al.*, 1992) suggested that the 840–850 cm^{-1} band of nontronites is similar to the 839–848 cm^{-1} band observed by Russell *et al.* (1970) and Cracium (1984) in montmorillonite and assigned by them to AlMgOH deformation. The presence of a small amount of Mg(II) in octahedral sites of sample SWa-1 and the apparently low intensity of the 846 cm^{-1} band (Table 2, Figure 2) are consistent with this assignment; but several earlier studies called into question the validity of this assignment. For instance, the intensity of the 844 cm^{-1} band in Garfield nontronite (Fialips *et al.*, 2002) is high even though the amounts of octahedral Mg and Al are much less in Garfield than in SWa-1. Alternative assignments of the 846 cm^{-1} band are Si–O (apical) stretching vibration (Russell *et al.*, 1979) or $(Fe)_2OH$ deformation (Stucki and Roth, 1976), but the attribution of this band is still being debated (*e.g.* Fialips *et al.*, 2002).

The IR spectra of the reduced SWa-1 in the *M*OH deformation range are presented in Figure 1. Each spectrum was decomposed in the 750–950 cm^{-1} range to visualize better the changes occurring upon reduction. Results of a possible decomposition for each spectrum are presented in Table 2, and representative spectra for the 10 and 30 min reduced samples are also shown in Figure 3. After 10 min of reduction, the 846 cm^{-1} band totally disappeared and all the other bands decreased significantly in intensity. The 875 and 822 cm^{-1} band remained almost stationary, but the 919 and 788 cm^{-1} bands apparently shifted down to 914 and 781 cm^{-1}, respectively (Table 2, Figures 1 and 3a). The 7 cm^{-1} shift of the 788 cm^{-1} band downward and its decrease in intensity are inconsistent with the assignment of this band to the Si–O vibration of a Si-rich admixture. If this band was due to such an admixture, its intensity would either increase or remain unchanged because the reduction process is unable to dissolve such a material without first altering the clay itself. Moreover, its position should be unrelated to Fe oxidation state. The behavior of this band is more likely to be related to an O–H vibrator connected to at least one Fe. Thus, in the case of SWa-1, this band could be due to FeMgOH groupings, even though this assignment for the band at 792 cm^{-1} in Garfield nontronite may be different (Fialips *et al.*, 2002). In the case of Garfield, this band

Table 2. Position ($\bar{\nu}$) and integrated area (A) of the component bands from the spectral deconvolution of the IR OH-deformation region reported in Figure 2 for unaltered (0 min) and ferruginous smectite (SWa-1) samples reduced for varying periods of time (10–240 min).

	0 min reduction		10 min reduction		30 min reduction		60 min reduction		240 min reduction	
	$\bar{\nu}$ (cm^{-1})	A (%)	$\bar{\nu}$ (cm^{-1})	A (%)	$\bar{\nu}$ (cm^{-1})	A (%)	$\bar{\nu}$ (cm^{-1})	A (%)	$\bar{\nu}$ (cm^{-1})	A (%)
1	919	14.2	914	6.4	911	5.4	910	3.6	910	2.8
2	875	36.8	873	26.6	874	16.8	869	10.2	864	9.0
3	846	9.2	–	–	–	–	–	–	–	–
4	822	19.2	821	16.1	827	7.2	835	2.7	835	1.5
5	788	10.0	781	5.3	781	0.5	–	–	–	–
Total:		89.4		54.4		29.9		16.5		13.3

Note: $0.02 \leqslant \chi^2 \leqslant 2.8$; $0.9997 \leqslant R^2 \leqslant 1.000$

may be the deformation range analogue of the 3532 cm^{-1} band that Fialips *et al.* (2002) observed in the stretching range, the origin of which is still uncertain. After 30 min of reduction the 781 cm^{-1} band almost disappeared, suggesting that the dehydroxylation of the FeMgOH groupings is almost complete (Table 2, Figure 3b). The three other remaining bands further decreased in intensity as reduction progressed, and the Fe_2OH band clearly shifted up to 827 cm^{-1} while the Al_2OH band apparently shifted slightly downward to 911 cm^{-1}. As the time of reduction increased up to 240 min, the decomposition of the spectra became more difficult and clearly much less accurate due to the very low intensity of the *M*−O−H deformation bands (*M* = Al, Mg, Fe) compared to the large contribution of the Si−O vibration band located at ~1000 cm^{-1}. However, results presented in Table 2 suggest that the band at 780−790 cm^{-1} totally disappeared within the first hour of reduction and that the Al_2OH, AlFeOH and Fe_2OH bands decreased in intensity with increasing reduction time, while also shifting to 910 cm^{-1} (down), 864 cm^{-1} (down), and 835 cm^{-1} (up), respectively.

The decrease in intensity of the *M*−O−H deformation bands (*M* = Mg, Al, or Fe) upon reduction reflects a progressive loss of OH groups, as already observed in several studies of other reduced nontronites (*e.g.* Stucki and Roth, 1976; Manceau *et al.*, 2000b; Fialips *et al.*, 2002). However, changes in the absorptivity of the *M*−O−H vibrations upon reduction could also partly explain these decreases in intensity. The shifts in *M*−O−H band positions could also be attributed in part to changes in the OH dipole orientation due to different electric field environments as a result of changes in Fe oxidation state and/or Fe rearrangement within the octahedral sheet. For instance, the reduction of Fe(III) to Fe(II) induces a deficit of charge on the apical oxygen (O_T) of the nearest tetrahedron which enhances attraction between O_T and the proton of the OH dipole, resulting in a change in the orientation of the OH dipole and the weakening of the O-H bond. However, the increasing overlap of the Si−O-stretching band in the 850−950 cm^{-1} range could cause the curve-fitting program to shift these bands artificially, especially the Al_2OH and AlFeOH bands which are closer to the Si−O region, due to an over estimation of the Si−O band width and/or Lorentzian/Gaussian ratio.

Another band was observed at 677 cm^{-1} in the unreduced sample (Figure 1), and is attributed to an Fe−O out-of-plane vibration (Farmer, 1974). As the time of reduction increased to 240 min, this band apparently shifted progressively downward to ~650 cm^{-1} and increased slightly in intensity. This behavior suggests that the properties of the SWa-1 Fe−O bonds (length and strength) are significantly and progressively modified upon reduction of ^{VI}Fe(III). No previous studies found such drastic movement in this band in reduced nontronites. Fialips *et al.* (2002) observed no modification

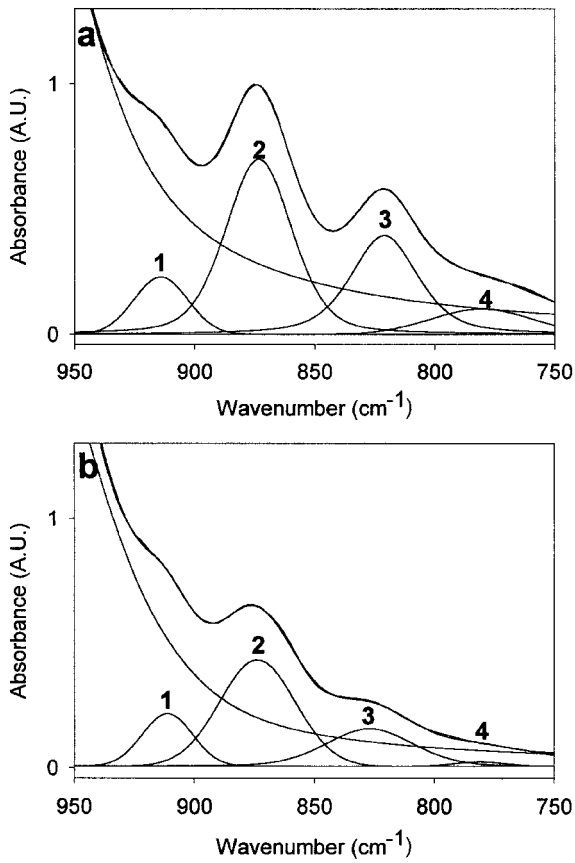

Figure 3. Deconvolution of the (a) 10 min and (b) 30 min reduced SWa-1 IR spectra into several components (see Table 2) in the OH-deformation range; experimental and calculated curves.

of the 672 cm^{-1} band of the Garfield nontronite, but did observe the appearance of a new band at 653 cm^{-1} after 240 min of reduction. They suspected a relationship between this new band and trioctahedral domains in highly-reduced Garfield. The fact that the 672 cm^{-1} of Garfield is stationary upon reduction indicates that the change in Fe oxidation state itself is not enough to explain the shift of this Fe−O deformation band to 650 cm^{-1} in SWa-1. This shift could actually be due to the appearance of a new band at ~650 cm^{-1}, as observed in Garfield, which progressively increases in intensity compared to the 677 cm^{-1} band. If the 653 cm^{-1} band is related to trioctahedral domains, the progressive increase in intensity of this band indicates that the formation of trioctahedral domains in SWa-1 begins within the first half hour of reduction and steadily increases, and that the distribution of such trioctahedral domains within the sheet (in clusters, orderly, or randomly) is probably different from Garfield.

The IR spectra of the unreduced, reduced and reduced-reoxidized samples (Figure 4) reveal important information regarding possible effects of reoxidation on *M*−O−H deformations and on the extent of reversibility after reduction. None of the reduced-reoxidized samples

exhibited the same spectra as the unreduced SWa-1. Thus, as already observed in previous studies of reduced-reoxidized nontronites (*e.g.* Komadel *et al.*, 1990; Heller-Kallai, 1997; Fialips *et al.*, 2002), structural changes occurring during reduction are only partially reversible, even if all the Fe(II) is reoxidized to Fe(III). The positions of some specific peaks were restored, however, regardless of the reduction time. The IR spectrum of the 60 and 240 min reduced and reoxidized SWa-1 were decomposed in the 750–950 cm^{-1} range using as input data the properties of the component bands obtained after deconvolution of the unaltered SWa-1 (Table 2). Results of possible deconvolutions are presented in Table 3. Note that the positions of the Al_2OH, AlFeOH and Fe_2OH deformation bands of SWa-1 were all restored upon reoxidation even after extensive reduction (Figure 4, Tables 2 and 3). The intensity of the 875 cm^{-1} band was mainly restored, especially after the shorter (10 and 30 min) reduction times (Figure 4). The 822 cm^{-1} band intensity was also partly restored but to a lesser extent than the 875 cm^{-1} band (Tables 2 and 3). Reoxidation failed to restore the 846 cm^{-1} band, regardless of the time of reduction (Figure 4, Table 3). And, whatever the time of reduction, the shoulder probably due to Fe(III)MgOH deformation mode was observed after reoxidation, except at ~780 cm^{-1} instead of ~792 cm^{-1} and more resolved compared to the unaltered SWa-1 (Figure 4, Table 3). Though the ~780 cm^{-1} band was never restored fully in intensity upon reoxidation, it is apparently most intense after the shortest reduction time (Figure 4, Table 3). Except for the 10 min reduced sample, reoxidation failed to restore the 677 cm^{-1} band to its original stature and position. This partial irreversibility demonstrates that, upon reduction, not only are transformations observed in the Fe-Al octahedral neighbors due to Fe(III) reduction to Fe(II) but also observed are some irreversible rearrangements of the octahedral cations.

IR spectra in the 800–1300 cm^{-1} region

The Si–O-stretching bands of the 0 to 240 min reduced samples are shown in Figure 5. For the unaltered SWa-1 (0 min reduction), the Si–O basal and apical stretching modes generated the intense band at 1036 cm^{-1} and the shoulder at 1107 cm^{-1}, respectively. From 10 to 240 min of reduction, the position of the 1036 cm^{-1} band shifted progressively down to 991 cm^{-1}, and the 1107 cm^{-1} shoulder shifted progressively down to ~1090 cm^{-1} and decreased in intensity compared to the 1000–1036 cm^{-1} band. Similar shifts have been reported for reduced nontronites and smectites

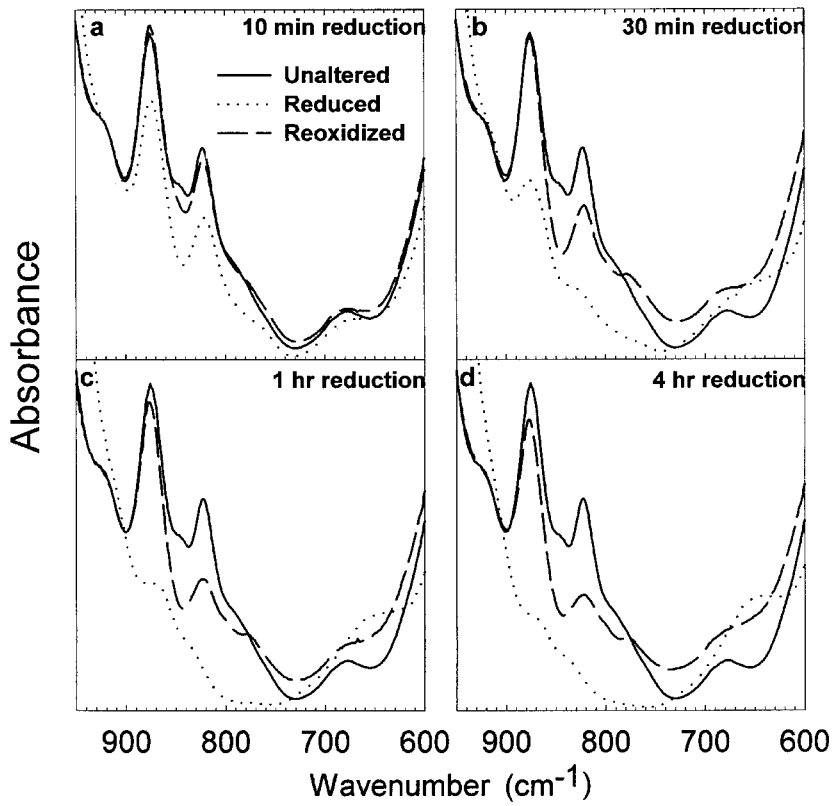

Figure 4. Normalized IR spectra in the OH-deformation region of the SWa-1 nontronite reduced over (a) 10 min, (b) 30 min, (c) 60 min, and (d) 240 min, then reoxidized. The spectrum of the initially unaltered SWa-1 is given in each plot for comparison.

Table 3. Position ($\bar{\nu}$) and integrated area (A) of the component bands from the spectral deconvolution of the IR OH-deformation region (see Figure 4) of the reoxidized forms of ferruginous smectite (SWa-1) samples reduced for 60 and 240 min.

60 min reduction		240 min reduction	
$\bar{\nu}$ (cm^{-1})	A (%)	$\bar{\nu}$ (cm^{-1})	A (%)
919	13.9	919	12.5
875	31.8	876	26.9
822	10.9	820	7.4
782	5.9	778	2.9
Total:	62.5		49.7

Note: χ^2 = 0.4-0.6; R^2 = 0.9997

(Stucki and Roth, 1976; Rozenson and Heller-Kallai, 1976a, 1976b; Komadel *et al.*, 1990; Yan and Stucki, 1999, 2000; Fialips *et al.*, 2002).

Regardless of the time duration of reduction, reoxidation failed to restore totally the shape and position of the overall envelope of the Si−O stretching modes (Figure 6). However, the Si−O basal stretching band of all the reduced samples moved in the direction of the unaltered sample to the same final position (*i.e.* 1027 cm^{-1}) upon reoxidation. By comparison, the more Garfield nontronite was reduced, the less its Si−O-stretching bands were restored upon reoxidation (Fialips *et al.*, 2002). While changes in the orientation of the clay film could affect the relative intensity of Si−O in-plane and out-of-plane vibrations, resulting in a few wavenumbers shift of the Si−O band, this is an unlikely explanation for the shifts in Si−O bands observed in these samples. The Si−O-stretching bands in the layers of self supporting films of reduced SWa-1, which are known to be less oriented than

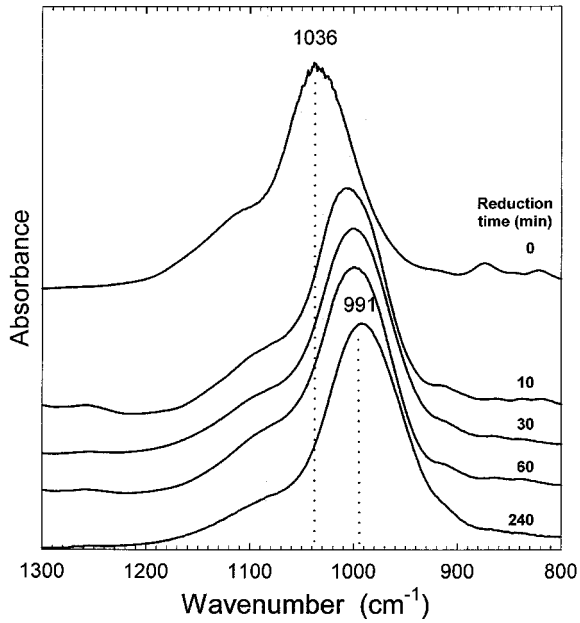

Figure 5. IR spectra in the Si−O-stretching region of the SWa-1 nontronite initially unreduced, and reduced with sodium dithionite for periods varying from 10 to 240 min.

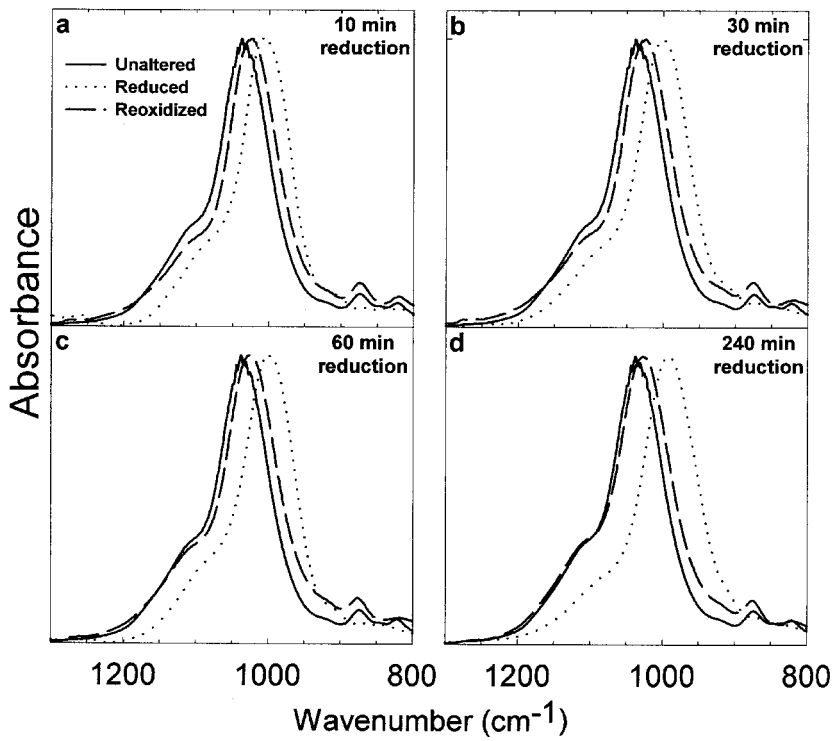

Figure 6. IR spectra in the Si−O-stretching region of the SWa-1 nontronite reduced for (a) 10 min, (b) 30 min, (c) 60 min, and (d) 240 min, then reoxidized. The spectrum of the initially unaltered SWa-1 is given in each plot for comparison.

those of Garfield (Manceau *et al.*, 2000a), shift by a similar amount (45 cm^{-1} down) to the Garfield nontronite (43 cm^{-1}, Fialips *et al.*, 2002). Further, a shift of 43–45 cm^{-1} is too large a shift to be explained simply by an orientation effect.

These variations in the Si–O band position and relative intensity confirm that changes in Fe oxidation state in the octahedral sheet strongly affect the structural properties of the tetrahedral sheet. These variations are at least partly connected with the changes in layer charge upon reduction (increase of layer charge) and reoxidation (decrease of layer charge; Madejová *et al.*, 1996; Komadel *et al.*, 1999; Fialips *et al.*, 2002). They could, however, also be generated by the formation of trioctahedral domains during the reduction process.

IR spectra in the 3000–3800 cm^{-1} region

The *M*–O–H-stretching bands (*M* = Mg, Al, or Fe) of the 0 to 240 min reduced samples change dramatically (Figure 7). For unaltered SWa-1 (0 min reduction), the overall *M*–O–H envelope was broad and non-symmetrical due to the presence of several component bands, as observed by Madejová *et al.* (1994). Our sample, however, was more extensively dried than the one used by Madejová *et al.* (1994), which allowed us to achieve a more accurate deconvolution (Figure 8; Table 4). Five OH-stretching bands in the range 3565–3652 cm^{-1} and two H–O–H-stretching bands at 3467 and 3231 cm^{-1} were necessary to obtain a satisfactory fit of the experimental spectrum (χ^2 = 4.92 and R^2 = 1.000). The integrated area of each OH-stretching component was normalized to the total area of all components and assignments for all bands are proposed (Table 4). The intense 3565 cm^{-1} band, attributed to $[Fe(III)]_2OH$-stretching modes, is always observed in the IR spectra of nontronites (Goodman *et al.*, 1976; Russell *et al.*, 1979; Fialips *et al.*, 2002). The 3652 cm^{-1} band is attributed to Al_2OH, though shifted upward by 20 to 30 cm^{-1} compared to data from Farmer and Russell (1964) and Goodman *et al.* (1976) for other smectites, and is well correlated with the peak at 921 cm^{-1} for Al_2OH deformation. The OH-stretching frequency in SWa-1 is slightly greater than in other nontronites, such as Garfield (Fialips *et al.*, 2002), because of less Al or Fe substitution in the tetrahedral sheet, and thus less attraction between the closest apical oxygens and the OH proton (Farmer and Velde, 1973; Farmer, 1974).

Table 4. Position ($\bar{\nu}$), integrated area (*A*), and assignment of the component bands from the spectral deconvolution of the IR OH-stretching region (Figures 7, 8) of unaltered ferruginous smectite (SWa-1).

Band	OH environment	$\bar{\nu}$ (cm^{-1})	*A* (%)
1	AlAlOH	3652	16.01
2	AlMgOH	3627	5.90
3	AlFeOH	3611	17.81
4	FeMgOH	3584	6.90
5	FeFeOH	3565	53.38
Total			100.00

Note: χ^2 = 4.92, R^2 = 1.0000

As noted above, the curve deconvolution solution found in the current study placed the OH-stretching bands consistently at a greater frequency by ~23 cm^{-1} (Table 4) compared to the solution proposed by Madejová *et al.* (1994). This difference may be attributed first to the fact that their spectra contained large water bands making precise corrections for the overlapping water bands very difficult, and second, their decomposition arbitrarily included two Al_2OH bands and two Fe_2OH bands, which were unnecessary in our solution (Figure 8, Table 4). Comparison of relative intensities of the component peaks reveals that the solution from the present study agrees perfectly with the chemical composition of the unaltered SWa-1 (1.08

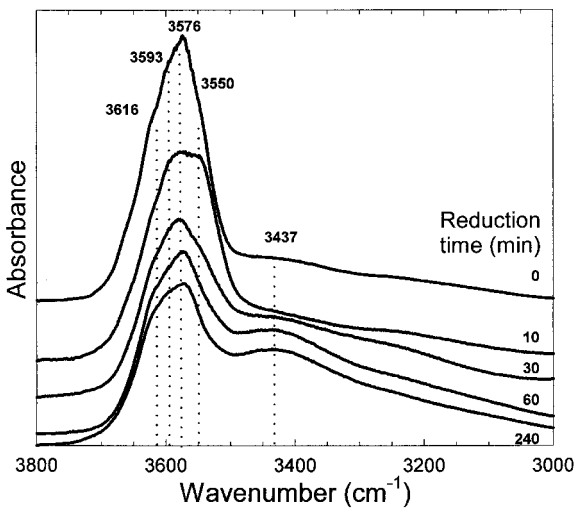

Figure 7. Normalized IR spectra in the OH-stretching region of the SWa-1 nontronite initially unreduced, and reduced with sodium dithionite for periods varying from 10 to 240 min.

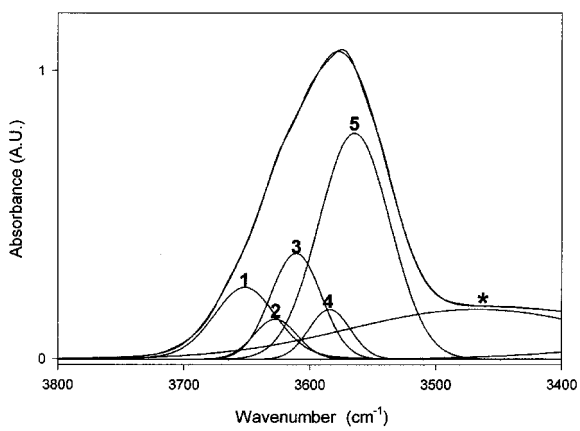

Figure 8. Deconvolution of the unaltered SWa-1 IR spectrum into several components (see Table 4) in the OH-stretching range; experimental and calculated curves.

^{VI}Al, 2.67 ^{VI}Fe, and 0.23 ^{VI}Mg per formula unit), assuming the absorptivity is the same for all *M*–O–H vibrators. This solution, moreover, indicates that 11, 57 and 32% of the ^{VI}Al atoms are neighbors to 1 ^{VI}Mg, 1 ^{VI}Al, and 1 ^{VI}Fe, respectively; but only 14 and 5% of the ^{VI}Fe atoms are adjacent to 1 ^{VI}Al and 1 ^{VI}Mg, respectively, while the remaining ^{VI}Fe atoms are adjacent to another ^{VI}Fe. Further, 46% of the ^{VI}Mg atoms are adjacent to 1 ^{VI}Al while 54% have 1 ^{VI}Fe neighbor. Thus, as proposed by Madejová *et al.* (1994) and Manceau *et al.* (2000a), the octahedral environments surrounding the OH groups of SWa-1 are mainly AlFe(III)OH and $[Fe(III)]_2OH$, the proportion of Fe-Fe pairs being greater than Al-Fe pairs. This agrees with observations in the NIR range (*i.e.* 4200–4600 cm^{-1}, Gates *et al.*, 2002) for the unreduced SWa-1. Low-intensity bands observed in the range 3200–3450 cm^{-1} for the unreduced SWa-1 (Figures 7 and 8) are due to adsorbed water (symmetrical and asymmetrical H_2O-stretching bands; Farmer, 1974).

After 10 min of reduction, the overall *M*–O–H-stretching band broadened significantly and decreased slightly in intensity (Figure 7). As the reduction time increased from 10 to 60 min, its shape and area changed progressively (Figure 7). To understand better the changes occurring during the reduction process, a systematic deconvolution of the IR spectra was performed. The spectra were first normalized to the total area of all the OH-stretching components in the unaltered SWa-1 to allow comparison of the band intensities. The properties of the OH-stretching component bands of the unaltered SWa-1 were used as input to begin the deconvolution of the 10 min reduced sample. An acceptable deconvolution (χ^2 = 10.10, R^2 = 1.000) was possible only after adding a new band at 3543 cm^{-1} (Table 5; Figure 9a). This band is attributed to a combination of Fe(III)Fe(II)OH and possibly $[Fe(II)]_2OH$ groupings. The positions of the 3652, 3627, 3584 and 3565 cm^{-1} bands appeared to be unaffected, consistent with the assignment of the 3652 and 3627 cm^{-1} bands to Al_2OH and AlMgOH groupings, respectively. Evidently the ^{VI}Fe(III) atom next to

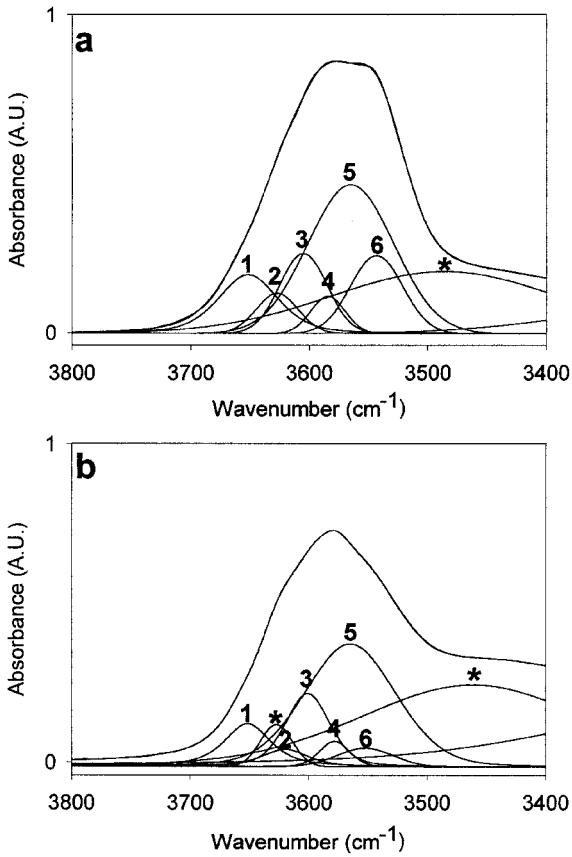

Figure 9. Deconvolution of the (a) 10 min and (b) 30 min reduced SWa-1 IR spectra into several components (see Table 5) in the OH-stretching range; experimental and calculated curves.

1 ^{VI}Mg was unreduced during 10 min of reduction, and a large proportion of ^{VI}Fe(III)^{VI}Fe(III) pairs also remained. The AlFeOH band, previously located at 3611 cm^{-1} for the unaltered SWa-1, shifted down to 3605 cm^{-1}, indicating that part of the ^{VI}Fe adjacent to ^{VI}Al was reduced to Fe(II), as an AlFe(II)OH band is expected to be at lower wavenumber than the AlFe(III)OH band. The sum of the relative areas of the 3565 and 3543 cm^{-1} bands equals 53% of the total,

Table 5. Position ($\bar{\nu}$) and integrated area (*A*) of the component bands from the spectral deconvolution of the IR OH-stretching region (see Figures 7, 9) of ferruginous smectite (SWa-1) samples reduced for periods varying between 10 and 240 min.

	10 min reduction		30 min reduction		60 min reduction		240 min reduction	
	$\bar{\nu}$ (cm^{-1})	*A* (%)	$\bar{\nu}$ (cm^{-1})	*A* (%)	$\bar{\nu}$ (cm^{-1})	*A* (%)	$\bar{\nu}$ (cm^{-1})	*A* (%)
1	3652	13	3652	8				
2	3627	5	3627	4	3620	22	3620	22
3	3605	12	3600	12				
4	3584	4	3578	3	3577	13	3574	13
5	3565	40	3565	37				
6	3543	13	3552	3	3552	20	3557	10
Total:		87		67		55		45

Note: $6.4 \leqslant \chi^2 \leqslant 12.3$; $0.993 \leqslant R^2 \leqslant 1.000$

which is similar to the relative area of the 3565 cm^{-1} band of the unaltered SWa-1, suggesting that no dehydroxylation and/or no change in the absorptivity of the Fe_2OH groupings occurred during the first 10 min of reduction. All other OH-stretching bands, however, decreased in relative area (Tables 4 and 5), especially the 3652 and 3605 cm^{-1} bands, reflecting a significant change in the absorptivity of the corresponding groupings and/or partial dehydroxylation.

The properties of the OH-stretching bands obtained after deconvolution of the 10 min reduced SWa-1 were used as input for the deconvolution of the 30 min reduced sample. One additional band at 3620 cm^{-1} was required for a successful fit. This band can be attributed to H–O–H-stretching vibrations of weakly-hydrogen bonded water molecules. An acceptable deconvolution (χ^2 = 7.11, R^2 = 0.9999) of the 30 min reduced sample (Table 5, Figure 9b) revealed that the relative area of each OH-stretching band decreased significantly compared to the 10 min reduced sample, indicating a greater loss of OH groups. This is confirmed also by the changes in the *M*–O–H deformation region (*i.e.* 750–950 cm^{-1}, Figures 1, 3, Table 2). The positions of the 3652, 3627 and 3565 cm^{-1} bands continued to be unaffected, supporting once again the attribution of the 3652 and 3627 cm^{-1} bands to Al_2OH and AlMgOH groupings, respectively, and indicating that a large proportion of $[Fe(III)]_2OH$ groupings are still present. The AlFeOH and FeMgOH bands shifted down to 3600 and 3578 cm^{-1}, respectively, indicating that a large proportion, if not all, of the ^{VI}Fe(III) atoms next to 1 ^{VI}Al or 1 ^{VI}Mg were reduced to Fe(II). The band attributed to a combination of Fe(III)Fe(II)OH- and $[Fe(II)]_2OH$-stretching modes was expected to keep its position or shift downward and to increase significantly in intensity upon reduction. This band, however, shifted only slightly upward compared to the 10 min reduced sample and decreased drastically in intensity. This behavior can be explained by extensive and preferential dehydroxylation of the Fe(III)Fe(II)OH and $[Fe(II)]_2OH$ groupings rather than $[Fe(III)]_2OH$ groupings.

The large water bands present in the 60 and 240 min reduced samples (Figure 7) precluded as reliable a deconvolution as obtained for the lesser reduced samples, so they were simply decomposed using the minimum number of components to obtain a satisfactory fit (low χ^2, R^2 closest to 1.000), *i.e.* three water bands (one low-intensity band at 3620 cm^{-1}, and two large and intense bands at ~3460 and 3260 cm^{-1}) and three structural OH-stretching components (Table 5). The intense component at 3620 cm^{-1} in both the 60 and 240 min reduced SWa-1 spectra may be due to the combination of Al_2OH- and AlMgOH-stretching vibrations. The relative area of this component band is, however, significantly greater than the sum of the relative areas of the individual Al_2OH and AlMgOH component bands of the 30 min reduced SWa-1, suggesting that a large change in the absorptivities occurred or, more likely, that a new band appeared in the range 3600–3650 cm^{-1}. If trioctahedral domains were formed within the octahedral sheet of SWa-1 upon reduction due to the migration of Fe(II) from *cis*- to *trans*- sites, such a new band would be expected for Fe(II)M_2OH at ~3610–3630 cm^{-1} (*M* = Fe(II), Mg or Al; Fialips *et al.*, 2002). Though the 30 min IR spectra are inconclusive on this point, the 60 min spectra are consistent with such an hypothesis. Cationic rearrangements within the octahedral sheet could be at least partly responsible for the decrease in intensity of the Fe*M*OH vibrations and the observed shifts in the Si–O–*M* bending vibrations (*M* = Fe(III) or Al).

The deconvolution of the 60 min reduced sample spectrum also required one component band at 3577 cm^{-1}, which can be attributed to a combination of AlFe(III)OH-, AlFe(II)OH- and Fe(II)MgOH-stretching vibrations. This component band, though keeping its relative area, shifted slightly down to 3574 cm^{-1} for the 240 min sample, indicating that some AlFe(III)OH groupings were still present in the 60 min reduced sample. A relatively intense component located at 3552 cm^{-1} was necessary to obtain a satisfactory deconvolution of the 60 min spectrum. This component can be attributed to a combination of Fe(III)Fe(II)OH and $[Fe(II)]_2OH$ vibrations, with $[Fe(II)]_2OH$ probably being the dominant grouping. After 240 min of reduction, this component band shifted slightly up and decreased drastically in relative area, probably due to dehydroxylation of the $[Fe(II)]_2OH$ groupings or to the formation of $[Fe(II)]_3OH$ (trioctahedral domains).

Dehydroxylation upon reduction was observed for Garfield nontronite (Roth and Tullock, 1973; Stucki and Roth, 1976, 1977; Lear and Stucki, 1985; Komadel *et al.*, 1995; Manceau *et al.*, 2000b; Fialips *et al.*, 2002); but, unlike Garfield, the SWa-1 smectite never completely lost its *M*–O–H-stretching bands, even after 240 min of reduction.

A plot of the total area of the OH-deformation and stretching bands (A_T) of SWa-1, normalized to the unaltered spectrum, as a function of structural Fe(II) content (Figure 10) revealed a linear decrease in band area with increasing time of Fe reduction. The corresponding number of OH groups lost (OH lost) was estimated by linear extrapolation assuming that A_T = 0 when OH lost = 4 (stoichiometric number of OH groups per unit-cell) and A_T = 100 when OH lost = 0, *i.e.*

$$A_T = \varepsilon l c = \varepsilon' c = 25c = 100 - 25c'$$

where the absorption coefficient ε' incorporates the path length *l* into the absorptivity ε, *c* is the number of OH per unit-cell, and *c*′ is the number of OH lost per unit-cell.

The amount of Fe(II) per unit-cell was also calculated based on the measured Fe(II) content, assuming the total Fe remained fixed during reduction, using the relation

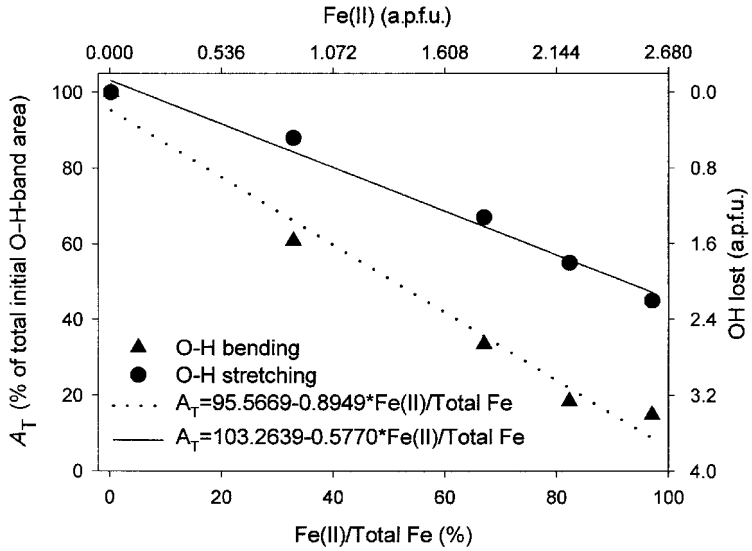

Figure10. Total area of the OH deformation and stretching bands, and corresponding calculated number of OH lost *vs.* the reduction level of the SWa-1 and the number of Fe(II) per formula unit.

$$\mathrm{Fe(II)} = \mathrm{k}\left[\frac{\mathrm{Fe(II)}}{\mathrm{Total\ Fe}}\right]$$

where the coefficient k is assumed to be constant (= 2.68 from the structural formula: Manceau *et al.*, 2000a) and converts the Fe(II):Total Fe ratio to atoms per unit-cell.

The areas of the OH-deformation and stretching bands decreased at different rates with increasing reduction, indicating that the absorptivities for these two modes differ. The OH-stretching band evidently is, however, the more reliable indicator of OH content because the A_T of the OH-deformation band approached zero after 240 min of reduction even though the OH-stretching band was still indicating the presence of OH. This further supports our hypothesis that the absorptivities of the different OH-deformation vibrators differ significantly from one another and probably change with increasing reduction time, thus explaining why the intensity of the AlFeOH-deformation band was more intense than that of the Fe_2OH band in the unaltered spectrum.

The use of the plot in Figure 10 as a first estimate of structural OH content may be possible but should be viewed with caution. For example, A_T of all OH-stretching bands estimates that ~0.8 OH molecules are lost per Fe(II) ion formed. The creation of trioctahedral domains upon migration of ^{VI}Fe(II) from *cis-* to *trans-*sites, however, produces a stretching band (Fe(II)M_2OH, M = Fe, Al or Mg) at ~3610–3630 cm^{-1} which has a much lower absorptivity compared to the other stretching component bands and thereby causes A_T to underestimate the amount of OH present (overestimates the loss of OH). In the 10 min reduced SWa-1, however, the number of trioctahedral domains created should be minimal, so in this case the transformation of scale from A_T to number of OH lost may be reliable. The value of OH lost/Fe(II) is 0.5. The value estimated by Lear and Stucki (1985) based on ^{3}H isotope exchange was 0.32. If we assume the latter to be correct, from the Beer-Lambert Law we can calculate an apparent absorptivity, ε_{app}', for the dioctahedral OH-stretching bands, using the relation

$$\varepsilon'_{\mathrm{app}} = \frac{25c'_1/n}{c'_2/n}$$

where $c_1'$and c_2' are the molecules of OH lost per n atoms of Fe(II) formed, as estimated from Figure 10 and Lear and Stucki (1985), respectively, giving a value for ε'_{app} of 39.06.

As time of reduction increased from 10 to 240 min, the ~3400 cm^{-1} and ~3200 cm^{-1} bands increased in intensity (Figure 7). These broad bands are due to H_2O molecules strongly H-bonded to the clay surface or to other H_2O molecules. As already proposed by several authors, these water molecules could be trapped inside large defect cavities created upon reduction by the migration of Fe(II) from *cis-* to neighboring *trans-*positions in the octahedral sheet (Manceau *et al.*, 2000b; Fialips *et al.*, 2002). The low intensity band located at 3620 cm^{-1}, which may be attributed to weakly-H-bonded water, was first observed in the spectrum of the 30 min reduced sample and increased slightly in area with reduction time.

The IR spectra of the unreduced, reduced and reduced-reoxidized samples in the M–O–H stretching region are shown in Figure 11. As already observed in the other IR spectral regions, none of the reduced-reoxidized samples exhibited the same spectra as the unreduced SWa-1, showing that structural changes occurring during Fe reduction are only partly reversible

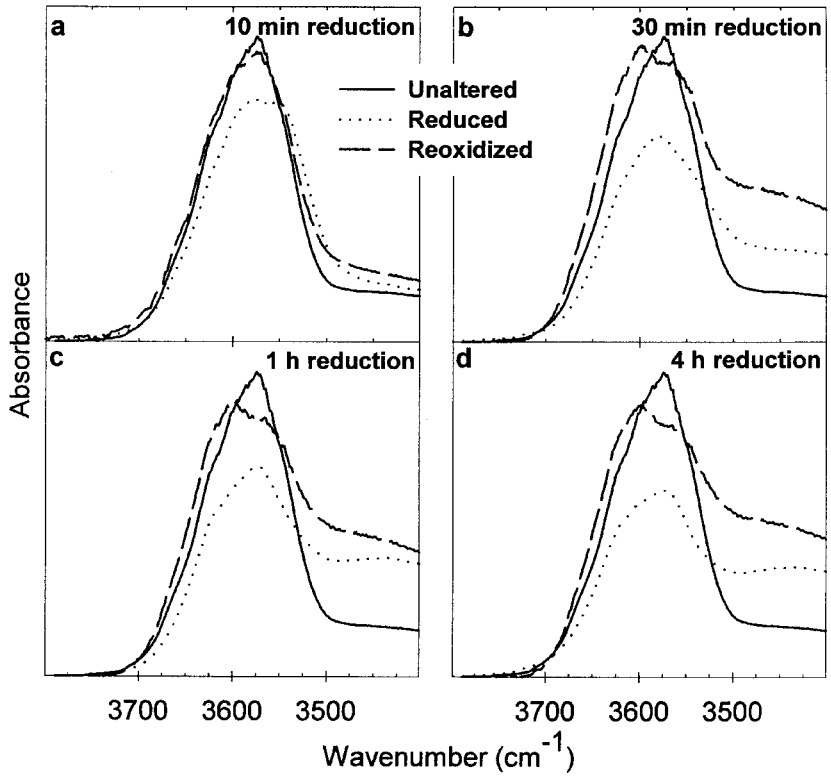

Figure 11. Normalized IR spectra in the OH-stretching region of the SWa-1 nontronite reduced for (a) 10 min, (b) 30 min, (c) 60 min, and (d) 240 min, then reoxidized. The spectrum of the initially unaltered SWa-1 is given in each plot for comparison.

though the reoxidation is almost complete (Fe(II) equals only 0.7 to 1.0% of total Fe; Table 1). For the 10 min reduced sample, however, the overall OH band was essentially restored to its original intensity and wavenumber upon reoxidation (Figure 11a). This is particularly obvious from the results of a possible deconvolution presented in Table 6. The IR spectrum of the 10 min reduced-reoxidized sample was first normalized to the total area of all the OH-stretching components in the unaltered SWa-1 to allow comparison, and the properties of the OH-stretching bands obtained after deconvolution of the unaltered SWa-1 spectrum were used as input parameters. After reoxidation, only 4% of the total area of the SWa-1 OH-stretching bands was not restored and all the bands which moved upon reduction (Table 6) shifted back to their original positions (Tables 4, 6). For all other reduction times, the loss of OH groups was restored to a large extent upon reoxidation but the overall OH band clearly shifted the maximum intensity to ~3600 cm^{-1} (Figure 11b,c,d). Considering the evidence from the OH-deformation IR region (*i.e.* better recovery of the AlFe(III)OH than the $[Fe(III)]_2OH$ deformation band upon reoxidation), this shift could be due to a low recovery of the $[Fe(III)]_2OH$ environment rather than enhancement of the number of AlFe(III) pairings.

To check this hypothesis, the IR spectrum of the 30 min reduced-reoxidized sample was decomposed after normalization to the total area of all the OH-stretching components in the unaltered SWa-1. The properties of the OH-stretching bands obtained after deconvolution of the unaltered SWa-1 spectrum were used as input parameters. Results of a possible deconvolution are presented in Table 6. These results indicate that 77% of the total area of the SWa-1 OH-stretching bands was restored upon reoxidation, but the AlFeOH band was almost fully restored while only 72% of the relative area of the Fe_2OH band was restored (Tables 4 and 6). A low recovery of the $[Fe(III)]_2OH$ band can occur in one of two ways: first, the rehydroxylation of these sites could be less complete

Table 6. Position ($\bar{\nu}$) and integrated area (A) of the component bands from the spectral deconvolution of the IR OH-stretching region of the reoxidized forms of ferruginous smectite (SWa-1) samples reduced for 10 and 30 min.

10 min reduction		30 min reduction	
$\bar{\nu}$ (cm^{-1})	A (%)	$\bar{\nu}$ (cm^{-1})	A (%)
3652	15	3652	13
3627	6	3627	5
3609	18	3600	17
3584	5	3578	4
3564	52	3565	38
Total:	96		77

Note: $\chi^2 \leqslant 27$; $R^2 \geqslant 0.999$

than for the other octahedral environments; and second, redistribution of Fe (and Al) could have occurred during reduction. In particular, as proposed earlier, some Fe could have migrated from *cis*- to *trans*- positions upon reduction (Manceau *et al.*, 2000b; Fialips *et al.*, 2002), leading to the formation of trioctahedral clusters. These migrations of Fe could be selective, Fe from Fe-Fe pairs being more involved than Fe from Al-Fe pairs. Even if all Fe(II) were reoxidized to Fe(III), reoxidation fails to reverse these structural changes and the cations are redistributed into a different configuration than found in the unreduced SWa-1.

Contrary to reduced Garfield nontronite (Fialips *et al.*, 2002), the tightly-bound H_2O band (~3400 cm^{-1}) of reduced SWa-1 smectite was retained during reoxidation. The water bands even increased in intensity, suggesting either that the drying method was less efficient than for the reduced samples or that more water was trapped within the clay structure.

CONCLUSIONS

The present observations in the IR range of O–H deformation, O–H stretching and Si–O stretching confirm that major changes occur within the structure of ferruginous smectite (SWa-1 sample) upon reduction. These changes affect both the octahedral and tetrahedral sheets of the clay and must be regarded as being only partially reversible. In particular, the migration of Fe from *cis*- to *trans*- positions within the octahedral sheet upon reduction is indicated and partly explains both the drastic variations in the OH deformation, OH-stretching, and Si–O-stretching bands upon reduction and their irreversibility. These rearrangements generate trioctahedral domains, as well as defect cavities, within the octahedral sheet during reduction with sodium dithionite at 70°C. Reoxidation of virtually all structural Fe(II) to Fe(III) restores some, but not all, of the original cationic arrangements.

ACKNOWLEDGMENTS

The authors gratefully acknowledge financial support for this work from the USDA National Research Initiative Program (Grant 93-37102-8957), DOE NABIR Program (DOE FSU F48792), International Arid Lands Consortium (Grant 00RO1) and Binational Agricultural Research and Development Program (BARD).

REFERENCES

Anderson, W.L. and Stucki, J.W. (1979) Effect of structural Fe^{2+} on visible absorption spectra of nontronite suspensions. *Proceedings of the 6th International Clay Conference, Oxford* (M.M. Mortland and V.C. Farmer, editors). Elsevier, Oxford, UK and Amsterdam, 75–83.

Chen, S.Z., Low, P.F. and Roth, C.B. (1987) Relation between potassium fixation and the oxidation state of octahedral Fe. *Soil Science Society of America Journal*, **51**, 82–86.

Cracium, C. (1984) Influence of the Fe^{3+} for Al^{3+} octahedral substitutions on the IR spectra of montmorillonite minerals. *Spectroscopy Letters*, **17**, 579–590.

Drits, V.A. and Manceau, A. (2000) A model for the mechanism of Fe^{3+} to Fe^{2+} reduction in dioctahedral smectites. *Clays and Clay Minerals*, **48**, 185–195.

Ernstsen, V., Gates, W.P. and Stucki, J.W. (1998) Microbial reduction of structural iron in clays – A renewable source of reduction capacity. *Journal of Environmental Quality*, **27**, 61–76.

Farmer, V.C. (1974) *The Infrared Spectra of Minerals*. Monograph **4**, Mineralogical Society, London, 344 pp.

Farmer, V.C. and Russell, J.D. (1964) The infrared spectra of layer silicates. *Spectrochimica Acta*, **20**, 1149–1173.

Farmer, V.C. and Velde, B. (1973) Effects of structural order and disorder on the infrared spectra of brittle micas. *Mineralogical Magazine*, **39**, 282–288.

Favre, F., Tessier, D., Abdelmoula, M., Genin, J.M., Gates, W.P. and Boivin, P. (2002) Iron reduction and changes in cation exchange capacity in intermittently waterlogged soil. *European Journal of Soil Science*, **53**, 175–184.

Fialips, C.I., Huo, D., Yan, L., Wu, J. and Stucki, J.W. (2002) Effect of iron oxidation state on the IR spectra of Garfield nontronite. *American Mineralogist*, **87**, 630–641.

Gates, W.P., Slade, P.G., Manceau, A. and Lanson, B. (2002) Site occupancies by iron in nontronites. *Clays and Clay Minerals*, **50**, 223–239.

Goodman, B.A., Russell, J.D., Fraser, A.R. and Woodhams, F.W.D. (1976) A Mössbauer and IR spectroscopic study of the structure of nontronite. *Clays and Clay Minerals*, **24**, 53–59.

Heller-Kallai, L. (1997) Reduction and reoxidation of nontronite: the data reassessed. *Clays and Clay Minerals*, **45**, 476–479.

Hunter, D.B., Gates, W.P., Bertsch, P.M. and Kemner, K.M. (1999) Degradation of tetraphenylboron at hydrated smectite surfaces studied by time resolved IR and X-ray adsorption spectroscopies. Pp. 282–300 in: *Mineral-water Interfacial Reactions: Kinetics and Mechanisms* (D.L. Sparks and T.J. Grundl, editors). ACS Symposium Series, **715**. American Chemical Society, Washington, D.C.

Huo, D. (1997) Infrared study of oxidized and reduced nontronite and Ca-K competition in the interlayer. Ph.D. thesis, University of Illinois, Champaign-Urbana, 139 pp.

Jackson, M.L. (1979) *Soil Chemical Analysis – Advanced Course,* 2nd edition. Madison, Wisconsin, 895 pp.

Khaled, E.M. and Stucki, J.W. (1991) Fe oxidation state effects on cation fixation in smectites. *Soil Science Society of America Journal*, **55**, 550–554.

Komadel, P. and Stucki, J.W. (1988) Quantitative assay of minerals for Fe^{2+} and Fe^{3+} using 1,10-phenanthroline: III. A rapid photochemical method. *Clays and Clay Minerals*, **36**, 379–381.

Komadel, P., Lear, P.R. and Stucki, J.W. (1990) Reduction and reoxidation of nontronite: extent of reduction and reaction rates. *Clays and Clay Minerals*, **38**, 203–208.

Komadel, P., Madejová, J. and Stucki, J.W. (1995) Reduction and reoxidation on nontronite: questions of reversibility. *Clays and Clay Minerals*, **45**, 105–110.

Komadel, P., Madejová, J. and Stucki, J.W. (1999) Partial stabilization of Fe(II) in reduced ferruginous smectite by Li fixation. *Clays and Clay Minerals*, **47**, 458–465.

Lear, P.R. and Stucki, J.W. (1985) Role of structural hydrogen in the reduction and reoxidation of Fe in nontronite. *Clays and Clay Minerals*, **33**, 539–545.

Lear, P.R. and Stucki, J.W. (1987) Intervalence electron transfer and magnetic exchange in reduced nontronite. *Clays and Clay Minerals*, **35**, 373–378.

Lear, P.R. and Stucki, J.W. (1989) Effects of Fe oxidation state on the specific surface area of nontronite. *Clays and Clay Minerals*, **37**, 547–552.

Madejová, J., Komadel, P. and Čičel, B. (1994) Infrared study of octahedral site populations in smectites. *Clay Minerals*, **29**, 319–326.

Madejová, J., Bujdák, J., Gates, W.P. and Komadel, P. (1996) Preparation and infrared spectroscopic characterization of reduced-charge montmorillonite with various Li contents. *Clay Minerals*, **31**, 223-241.

Manceau, A., Lanson, B., Drits, V.A., Chateigner, D., Gates, W.P., Wu, J., Huo, D. and Stucki, J.W. (2000a) Oxidation-reduction mechanism of iron in dioctahedral smectites. 1. Structural chemistry of oxidized reference nontronites. *American Mineralogist*, **85**, 133–152.

Manceau, A., Lanson, B., Drits, V.A., Chateigner, D., Wu, J., Huo, D., Gates, W.P. and Stucki, J.W. (2000b) Oxidation-reduction mechanism of iron in dioctahedral smectites. 2. Structural chemistry of reduced Garfield nontronites. *American Mineralogist*, **85**, 153–172.

Nzengung, V.A., Castillo, R.M., Gates, W.P. and Mills, G.L. (2001) Abiotic transformation of perchloroethylene in homogeneous dithionite solution and in suspensions of dithionite-treated clay minerals. *Environmental Science and Technology*, **35**, 2244–2251.

Petit, S., Prot, T., Decarreau, A., Mosser, C. and Toledo-Groke, M.C. (1992) Crystallochemical study of a population of particles in smectites from a lateritic weathering profile. *Clays and Clay Minerals*, **40**, 436–445.

Roth, C.B. and Tullock, R.J. (1973) Deprotonation of nontronite resulting from chemical reduction of structural Fe(III). *Proceedings of the International Clay Conference, Madrid* (J.M. Serratosa and A. Sanchez, editors). Division de Ciencias, Madrid, 107–114.

Roth, C.B., Jackson, M.L. and Syers, J.K. (1969) Deferration effect on structural ferrous-ferric iron ratio and CEC of vermiculites and soils. *Clays and Clay Minerals*, **17**, 253–264.

Rozenson, I. and Heller-Kallai, L. (1976a) Reduction and oxidation of Fe(III) in dioctahedral smectites. 1: reduction with hydrazine and dithionite. *Clays and Clay Minerals*, **24**, 271–282.

Rozenson, I. and Heller-Kallai, L. (1976b) Reduction and oxidation of Fe(III) in dioctahedral smectites. 2: reduction with sodium sulphide solutions. *Clays and Clay Minerals*, **24**, 283–288.

Russell, J.D., Farmer, V.C. and Velde, B. (1970) Replacement of OH by OD in layer silicates and identification of the vibrations of these groups in infrared spectra. *Mineralogical Magazine*, **37**, 869–879.

Russell, J.D., Goodman, B.A. and Fraser, A.R. (1979) Infrared and Mössbauer studies of reduced nontronites. *Clays and Clay Minerals*, **27**, 63–71.

Serratosa, J.M. (1960) Dehydration studies by I.R. spectroscopy. *American Mineralogist*, **45**, 1101–1104.

Shen, S., Stucki, J.W. and Boast, C.W. (1992) Effects of structural Fe reduction on the hydraulic conductivity of Na-smectite. *Clays and Clay Minerals*, **22**, 381–386.

Stubican, V. and Roy, R. (1961) A new approach to assignment of infra-red absorption bands in layer-structure silicates. *Zeitschrift für Kristallographie*, **15**, 200–214.

Stucki, J.W. (1981) The quantitative assay of minerals for Fe^{3+} and Fe^{2+} using 1,10-phenanthroline: II. A photochemical method. *Soil Science Society of America Journal*, **45**, 638–641.

Stucki, J.W. and Roth, C.B. (1976) Interpretation of infrared spectra of oxidized and reduced nontronite. *Clays and Clay Minerals*, **24**, 293–296.

Stucki, J.W. and Roth, C.B. (1977) Oxidation-reduction mechanism for structural Fe in nontronite. *Soil Science Society of America Journal*, **41**, 808–814.

Stucki, J.W., Golden, D.C. and Roth, C.B. (1984a) Preparation and handling of dithionite-reduced smectite suspensions. *Clays and Clay Minerals*, **32**, 191–197.

Stucki, J.W., Golden, D.C. and Roth, C.B. (1984b) Effects of reduction and reoxidation of structural Fe on the surface charge and dissolution of dioctahedral smectites. *Clays and Clay Minerals*, **32**, 350–356.

Stucki, J.W., Low, P.F., Roth, C.B. and Golden, D.C. (1984c) Effects of oxidation state of octahedral Fe on clay swelling. *Clays and Clay Minerals*, **32**, 357–362.

Stucki, J.W., Bailey, G.W. and Gan, H. (1996) Oxidation-reduction mechanisms in iron-bearing phyllosilicates. *Applied Clay Science*, **10**, 417–430.

Stucki, J.W., Wu, J., Gan, H., Komadel, P. and Banin, A. (2000) Effects of iron oxidation state and organic cations on dioctahedral smectite hydration. *Clays and Clay Minerals*, **48**, 290–298.

Wu, J., Low, P.L. and Roth, C.B. (1989) Effects of octahedral-iron reduction and swelling pressure on interlayer distances in Na-nontronite. *Clays and Clay Minerals*, **37**, 211–218.

Yan, L. and Stucki, J.W. (1999) Effects of structural Fe oxidation state on the coupling of interlayer water and structural Si-O stretching vibrations in montmorillonite. *Langmuir*, **15**, 4648–4657.

Yan, L. and Stucki, J.W. (2000) Structural perturbations in the solid-water interface of redox transformed nontronite. *Journal of Colloid and Interface Science*, **225**, 429–439.

(*Received 23 April 2001; revised 5 March 2002; Ms 540*)